Volcanic tremor associated with eruptive activity at Bromo volcano

Ellen Gottschämmer
Geophysical Institute, University of Karlsruhe, Germany

Abstract
Three broadband stations were deployed on Bromo volcano, Indonesia, from September to December 1995. The analysis of the seismograms shows that the signals produced by the volcanic sources cover the frequency range from at least 25 Hz down to periods of several minutes and underlines, therefore, the importance of broadband recordings. Frequency analysis reveals that the signal can be divided into four domains. In the traditional frequency range of volcanic tremor (1-10 Hz) sharp transitions between two distinct values of the tremor amplitude can be observed. Additional tremor signal including frequencies from 10 to 20 Hz could be found during late November and early December. Throughout the whole experiment signals with periods of some hundred seconds were observed which are interpreted as ground tilts. For these long-period signals a particle motion analysis was performed in order to estimate the source location. Depth and radius can be estimated when the source is modelled as a sudden pressure change in a sphere. The fourth frequency range lies between 0.1 and 1 Hz and is dominated by two spectral peaks which are due to marine microseism. The phase velocity and the direction of wave propagation of these signals could be determined using the tripartite-method.

Key words *volcanic tremor – broadband seismology*

1. Introduction

Although Mt. Bromo has frequently been active in historical times with 50 known eruptions since 1804 (Wunderman *et al.*, 1995a), it has only rarely been the subject of scientific investigations. After a decade of quiescence it started being active again in March 1995 and showed a period of even stronger activity starting in September 1995 with major ash cloud eruptions. The eruptive activity was accompanied by high tremor activity (Wunderman *et al.*, 1995b) superimposed by signals with periods of some hundred seconds.

Mailing address: Dr. Ellen Gottschämmer, Geophysikalisches Institut der Universität Karlsruhe, Hertzstraße 16, 76187 Karlsruhe, Germany; e-mail: ego@gpiwap4.physik.uni-karlsruhe.de

Generally the spectra of volcanic tremor are dominanted by frequencies around 1-10 Hz. On many volcanoes (among others Semeru, Lascar, Galeras) harmonic tremor could be observed. The spectra in those consist of a few sharp peaks at frequencies which are integer multiples of a fundamental frequency. They can be found independently of the recording site and must, therefore, be produced by resonating sources (Schlindwein *et al.*, 1995; Benoit and McNutt, 1997). On other volcanoes (for example Stromboli) the narrow peaks observed at individual stations and even components are mainly dominated by path effects. Summing up the amplitude-spectra recorded at many different sites results in a broad bulge with no notable single peak frequencies (Mohnen and Schick, 1996). The shape of this bulge though is due to the volcanic source.

Volcanic tremor has been investigated for many years, but due to the lack of broadband field-seismometers the investigations have always been restricted to the frequency band above 1 Hz. Recently, investigation of volcanic shocks

could be combined with investigation of low frequency volcanic signals as shown for Stromboli (Dreier *et al.,* 1994; Neuberg *et al.,* 1994; Wielandt and Forbriger, 1999; Kirchdörfer, 1999). On Bromo, volcanic tremor was accompanied by long-period signals.

A review of different types of volcanic tremors and theories of volcanic tremor source dynamics can be found in McNutt (1994) and in other articles in this volume.

2. Seismic experiment

From September to December 1995 three seismic stations (LAW, RID, CUT) were deployed on Bromo volcano which is part of the chain of active volcanoes on Java. Mt. Bromo itself is a small pyroclastic cone with a wide crater (700 m in diameter) and the only volcano active within the 7-km-diameter Tengger Caldera. The seismic stations were deployed close to the crater at a distance of approximately 0. 5 to 1.5 km from the crater rim. Two more stations (JOW, LEK) were set up at Semeru volcano, about 20 km south of Bromo. Figure 1 shows all station locations. Each of the seismic stations consisted of a GURALP CMG 3T broadband-seismometer (3 components) buried in the ground at depths of approximately 1 m and a Lennartz MARS-88 data acquistition system with a sampling frequency of 62.5 Hz. The resulting response is flat with respect to ground velocity from 0.0083 Hz (120 s period) to 25 Hz after application of an anti-aliasing filter. All stations were equipped with a GPS time signal receiver. At Mt. Bromo the stations recorded continuously from September 21 to December 13 accumulating up to 15 Gbytes of data. This study however focuses on the analysis of data from six days for Bromo stations and one day for Semeru stations only. The experiment has been carried out jointly by the Volcanological Survey of Indonesia, Bandung, the University of Leeds, U.K., the University of Grenoble, France and the University of Stuttgart, Germany.

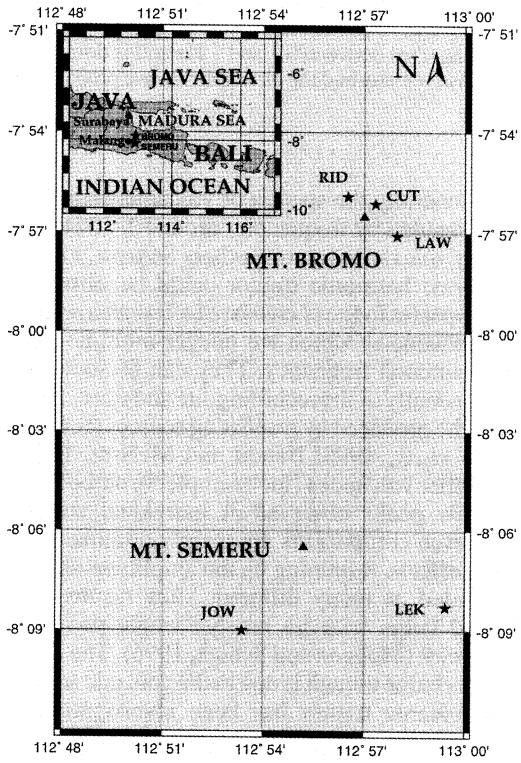

Fig. 1. Sketchmap showing the positions of the stations (★) at Mts. Bromo and Semeru.

3. The data

During the recording period Bromo showed high but intermittent eruptive activity accompanied by volcanic tremor. The most striking features were frequent and quick transitions between periods of high and low amplitude. It appears that the tremor source is stochastically switching between two phases or states: phase A with amplitudes higher by factors of about 4 than amplitudes during phase B.

The length of the periods in phases A and B varies from several minutes to several days and the transition between the two phases happens within one or two minutes. The transitions were found on all stations and components at the same time. Figure 2 shows a typical seismogram from October 27, with the amplitude corresponding to ground velocity in the passband of the system. Phases A and B can be easily

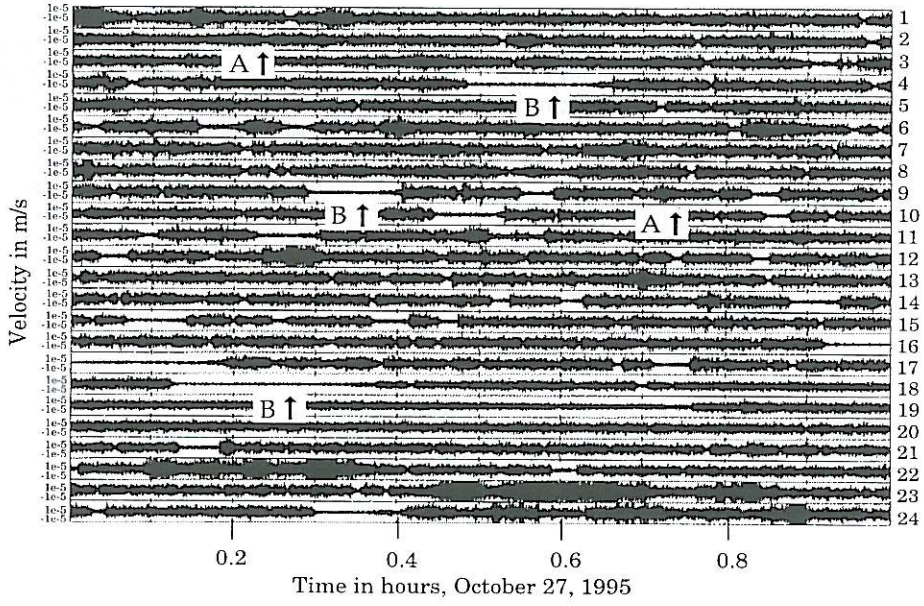

Fig. 2. Broadband velocity-seismogram for October 27, Station RID, Z-Component. One trace shows the registration of one hour. The top trace starts at midnight UT (7 a.m. local time). High tremor amplitudes (phase A) alternate with low amplitudes (phase B). The transitions between the two phases take only a few minutes.

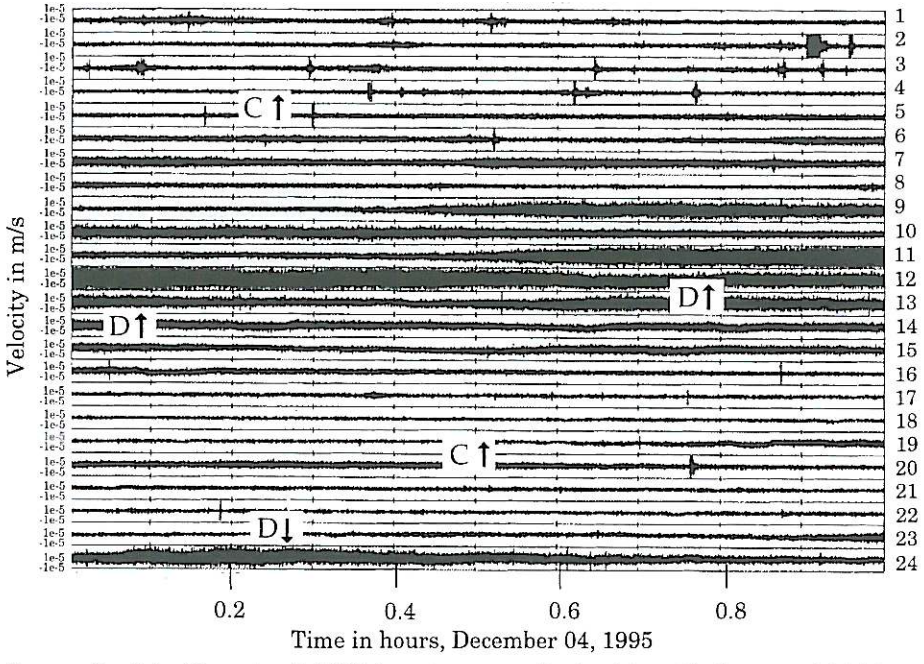

Fig. 3. Same as fig. 2 for December 4, 1995. Low tremor amplitudes (phase C) alternate with high amplitudes (phase D). The transitions between the two phases take about 10-20 min.

distinguished. While on the seismometers signals of phase A were recorded, the activity of Mt. Bromo was dominated by ash cloud eruptions (J. Neuberg, personal communication, 1996). During phase B only steam emissions could be seen.

A second type of tremor could be found only during late November and early December. It also consists of a phase with high and a phase with low amplitude. The transistions between the two phases however take about 10 to 20 min. This tremor also differs with respect to the spectral content from the tremor signals described above. The two phases are therefore called phase C and phase D (fig. 3).

Superimposed on the tremor, long-period signals could be observed. On December 04 the amplitudes of these signals on the horizontal components are as large as $\pm 10^{-4}$ m/s (fig. 4). On the vertical components the long-period signals are about 100 times smaller (fig. 3). In October and November the amplitudes of the long-period signals show values of only $\pm$ 1-2·10^{-7} m/s on the vertical components, and can therefore not be seen without filtering (as in fig. 2) .

The frequency range between 0.1 and 1 Hz is dominated by signals produced by marine microseisms. The signals are continuous for a period of at least some days and add therefore a constant value to the amplitude of the seismogram in fig. 2). Only when analysing the frequency content of the seismic signal can they be detected.

Consequently, the seismic signals recorded at Mt. Bromo can be split up into four groups according to their frequency content and will be

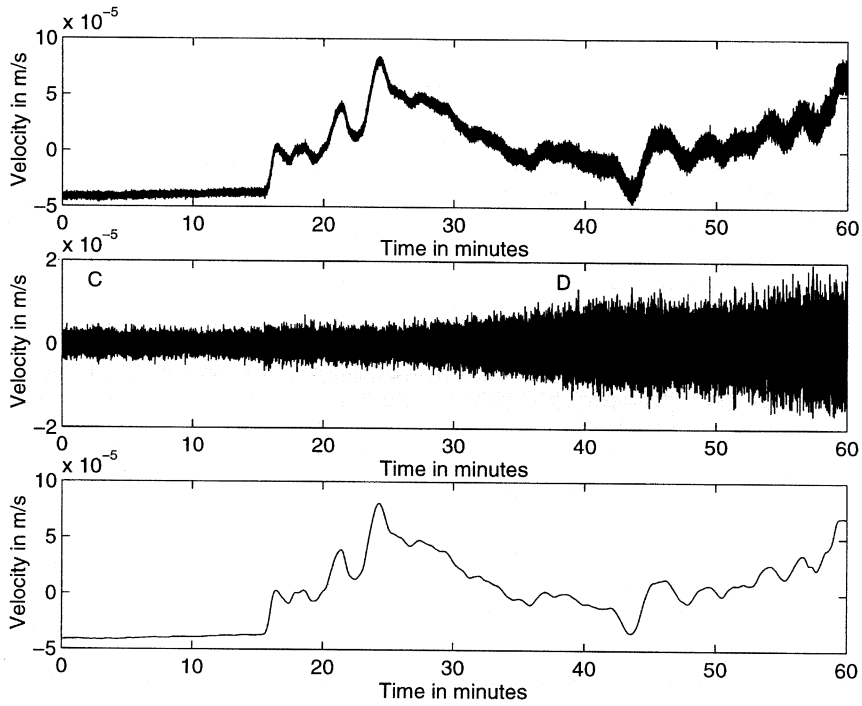

Fig. 4. Long-period signals on the velocity seismogram of December 4, 10-11 UT, Station LAW, E-Component. The velocity seismogram (unfiltered seismogram on top) is composed of long-period signals (bottom, low-pass 0.04 Hz) superimposed on an increasing tremor amplitude (middle, high-pass 0.04 Hz). The transition from phase C to phase D occurs more slowly (within 10 to 20 min) during the appearance of long period signals.

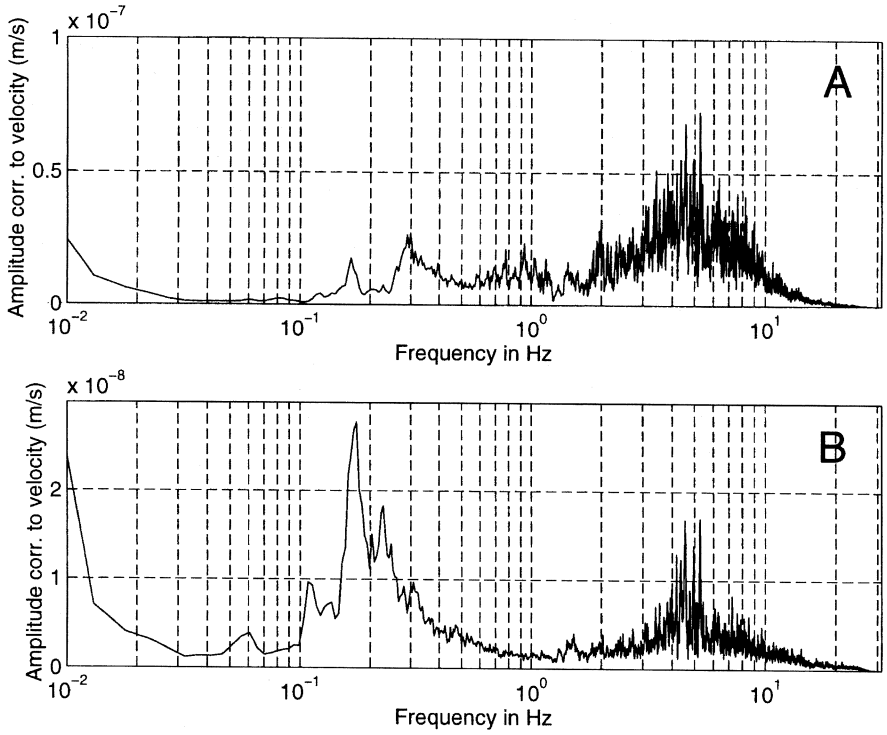

Fig. 5. Comparison of amplitude spectra for phase A (October 26, 20-21 UT, top) and phase B (October 15, 18-19 UT, bottom), Station RID, E-Component. The plotted values are running averages over 20 raw points. In the tremor frequency range the shape of the spectra is similar, however, the amplitude is much smaller during phase B. The peak near 0.2 Hz corresponds to the marine microseism.

analysed within the four different frequency ranges. These are, first, the traditional tremor in the frequency range from 1-10 Hz, secondly the two regions of high amplitudes around 0.15 Hz and 0.3-0.4 Hz, then, the long-period volcanic signals mainly recorded on the horizontal components, and, finally, the high frequency tremor in a range above 10 Hz.

4. Data analysis

4.1. *Traditional tremor range – frequencies from 1-10 Hz*

We first focus on tremor signals which are part of the frequency range from 1-10 Hz, as they could be observed during the whole recording period. In the seismogram two distinct phases can be identified: phase A with high tremor amplitudes and phase B with low amplitudes.

When analysing the frequency content it can be seen that the spectrum of phase A is predominated by the typical tremor frequencies from 1-10 Hz with amplitudes corresponding to velocities up to $7 \cdot 10^{-8}$ m/s. The spectrum of phase B shows lower amplitudes in this particular frequency range corresponding to velocities up to $1.7 \cdot 10^{-8}$ m/s (fig. 5) .

Generally, in the frequency domain the tremor on Mt. Bromo can be described as a broad bulge of several Hz bandwidth with a center frequency around 4-5 Hz. These tremor signals can be observed both during phases A and B, even though in the latter case the total amount of ener-

gy emitted is much smaller and the amplitudes, therefore, are approximately four times lower.

Since the shape of the spectrum in this frequency range is the same, the different behaviour during those two phases is probably not caused by a completely different source mechanism but just by a decreasing source intensity.

Superimposed on the broad bulge are small narrow peaks which, for each single recording site and independent of the signal amplitude, are stable for the whole recording period. Nevertheless these peaks cannot be found consistently at every station. This leads to the suspicion that they are not significant for the source, but depend on the recording site and its subsoil. A summation of the amplitude spectra however, as it was performed for Stromboli (Mohnen and Schick, 1996), does not smoothen the spectrum notably, because the number of different recording sites in this experiment is too small.

Even though the transitions between the two phases A and B take only a few minutes they are not sharp enough to allow the determination of arrival times at single stations. The tremor generally shows no significant wave forms (Neuberg and Wahyudi, 1991). Neither can the time-differences be determined by a cross-correlation, because the distance between the single stations is too small to obtain reasonable results. Particle motion analysis does not indicate any prefered direction of polarization which makes it impossible to determine the direction of the arriving waves. However, an attempt can be made to determine the tremor source, using amplitude information of at least three stations (Gottschämmer, submitted to JVGR, 1998). Independent of the phase (A or B), the tremor source (indicated by dots calculated for different time periods) is located in the north-western part of the crater (fig. 6) .

During some days around mid November a single peak could be observed at 1.25 Hz in addition to the tremor activity. Figure 7 shows amplitude-spectra from stations LAW, RID and CUT recorded at November 16, 10-11 UT. The outstanding peak at 1.25 Hz can be found on all three stations for several days. Figure 8 shows amplitude spectra for the Z, N and E-component recorded at the same time on station LAW. The peak is present on all three components and had also been observed with 1-Hz-seismometers in March and early September 1995 (Triastuty, 1997). This peak was only found during high amplitude tremor (phase A) and was possibly generated by resonances of a magma or gas filled dike or crack (Dahm, 1991).

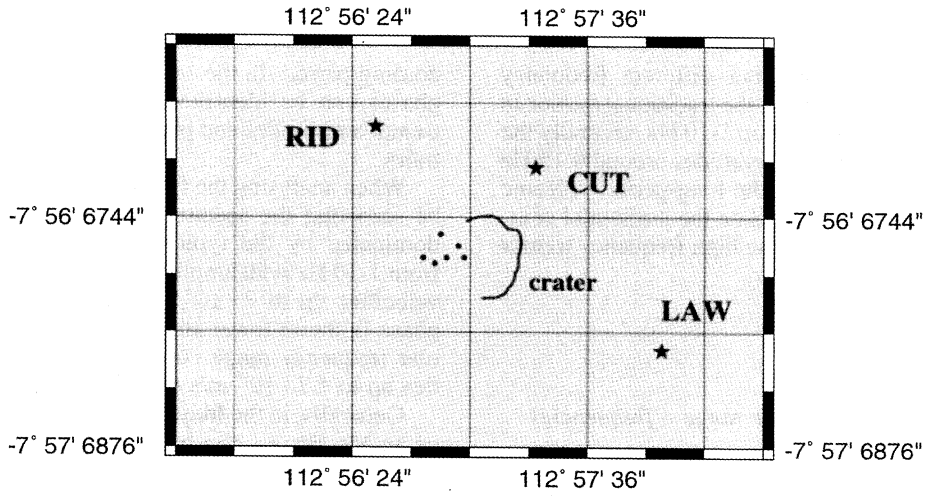

Fig. 6. Sketchmap of the crater region showing the positions of the tremor sources calculated from amplitudes for different time windows each with the length of one hour. The source locations are indicated by dots.

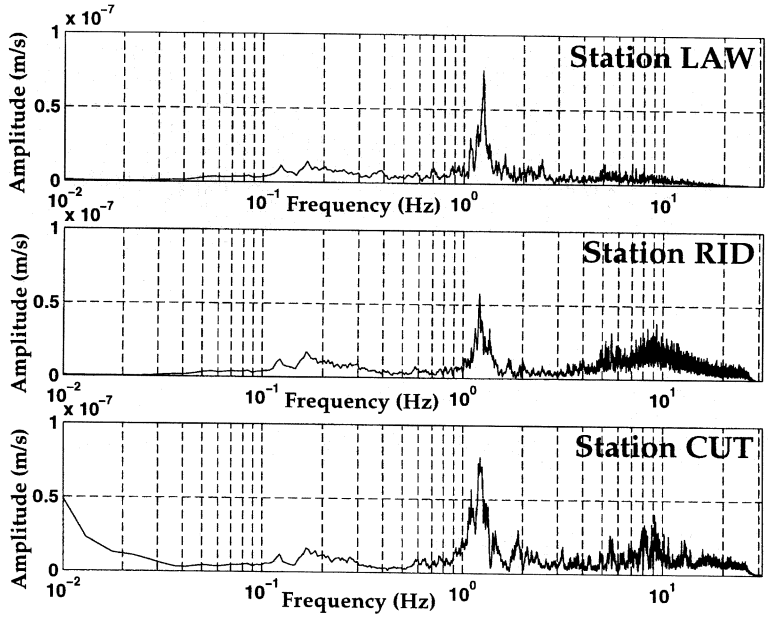

Fig. 7. Amplitude spectra for phase A, November 16, 10-11 UT (from top) Station LAW, RID and CUT, Z-Component. The peak at around 1.25 Hz is dominant on all of the stations. The plotted values are running averages over 20 raw points.

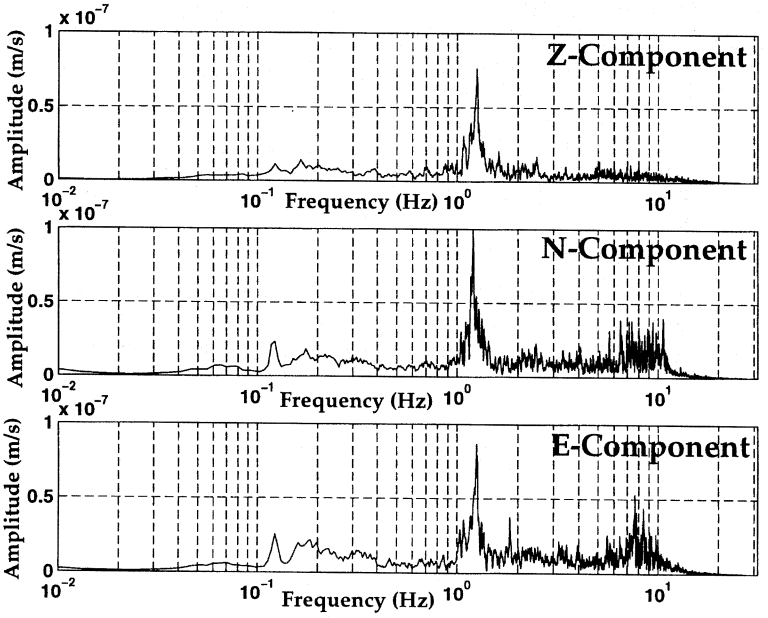

Fig. 8. Amplitude spectra for phase A, November 16, 10-11 UT, Station LAW, Z, N and E-Component (from top). The peak at around 1.25 Hz is dominant on all components. The plotted values are running averages over 20 raw points.

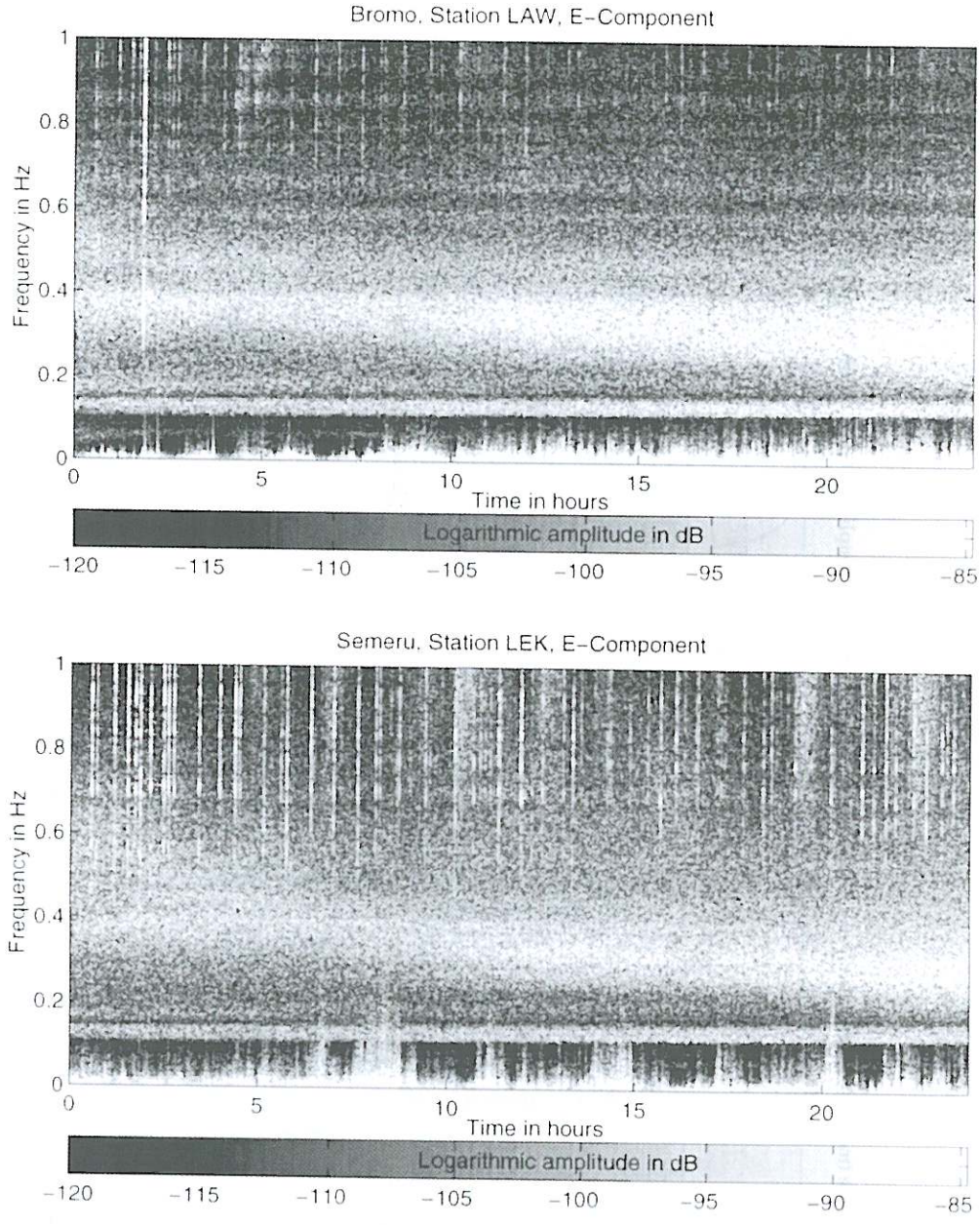

Fig. 9. Spectrograms for December 4, Stations LAW, E-Component (top) and LEK, E-Component (bottom). Apart from the microseism ridge at around 0.15 Hz a band around 0.3-0.4 Hz calls for attention. This band slowly decreases its center frequency and broadens towards the end of the day. Note that both bands have similar amplitudes near both volcanoes. The vertical streaks in both spectrograms behave differently. They are caused by volcanic shocks at the two volcanoes (Gottschämmer, 1998).

4.2. *Marine microseism – frequency range from 0.1-1 Hz*

This frequency range is dominated by marine microseism. Figure 9 shows on top a spectrogram from December 04 (station LAW, E-component) where two ridges of high spectral amplitudes attract attention. One of the ridges is found between 0.3 and 0.4 Hz on all stations and components. During this day the center frequency of this band decreases from 0.37 Hz to 0.32 Hz and the band gets broader. Comparing the signal with data from Mt. Semeru from the same time period, it can clearly be seen that this signal is present there as well (fig. 9, bottom) having approximately the same amplitude.

If the signal was emitted by either one of the two volcanoes the signal amplitude would have to be much higher on the spectrograms from this particular volcano. The similar values of the amplitudes on both spectrograms lead to the conclusion that the distance to the source is approximately the same for all stations.

Below this broad ridge a narrower one can be seen at around 0.15 Hz. This latter ridge is composed of frequencies typical for marine microseism. For this ridge the center frequency slowly increases. Furthermore it is notable that the marine microseism could be recorded during the whole recording time, whereas the signal at around 0.3-0.4 Hz only occured during some days around December 04 and October 26. Nevertheless, the fact that the signal has a period of about 3 s makes it likely that it is caused by a different source of sea-microseism.

Especially when estimating the direction of wave propagation this becomes obvious. For the investigation the signals recorded at the stations LAW and RID (Bromo) and LEK and JOW (Semeru) were band-pass filtered between 0.22-0.5 Hz and afterwards cross-correlated with one another. The cross-correlations show well defined peaks at certain time delays τ_{apparent}. Figure 10 shows the cross-correlation of the signals recorded at stations LEK and RID. The time difference has been estimated graphically after calculating the envelope using a Hilbert transform (fig. 10, bottom). In this case the estimated time-difference amounts to 16 s with the signal arriving first at station LEK. For the cross-correlations of other station pairs time-differences amount to between 2.5 s (LAW-RID) and 13 s (LEK-LAW).

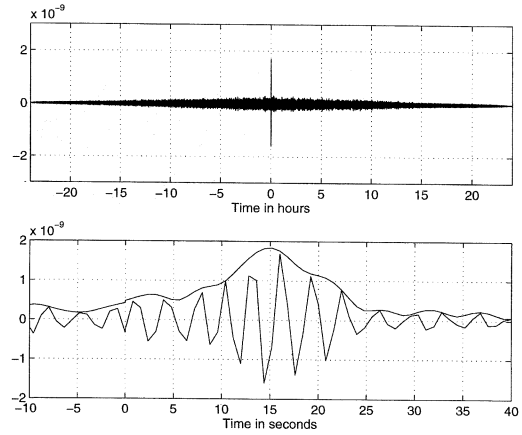

Fig. 10. Cross-correlation of signals recorded at station RID (Bromo) and LEK (Semeru) on December 4, 1995. The signal has been bandpass-filtered from 0.22-0.5 Hz. Correlation reveals a sharp peak (top). For the determination of time difference Δt the envelope of the cross-correlation has been calculated using the Hilbert-transform (bottom). For the two stations RID and LEK the time difference amounts to 16 s with LEK being early.

Assuming that these signals are produced by plane waves the direction of wave propagation can be estimated using the tripartite method (Knopoff *et al.*, 1967). For both triangles RID-JOW-LEK and LAW-JOW-LEK the calculations have been performed. The wave propagation azimuth is found between N 307°E and N 318°E as shown in fig. 11. Using the same assumptions as above the velocity of the waves in this limited frequency band could be on an average determined to 1.1 km/s. Satellite photos of the relevant days show storm centers in the Indian Ocean about half way between Java and Australia. The location of the storm center on December 4 is indicated in fig. 11. The same procedure has been performed for the narrow ridge at about 0.15 Hz in fig. 9. The data has been bandpass-filtered from 0.1 to 0.2 Hz and afterwards a cross-correlation has been calculated for data from two stations at a time. The

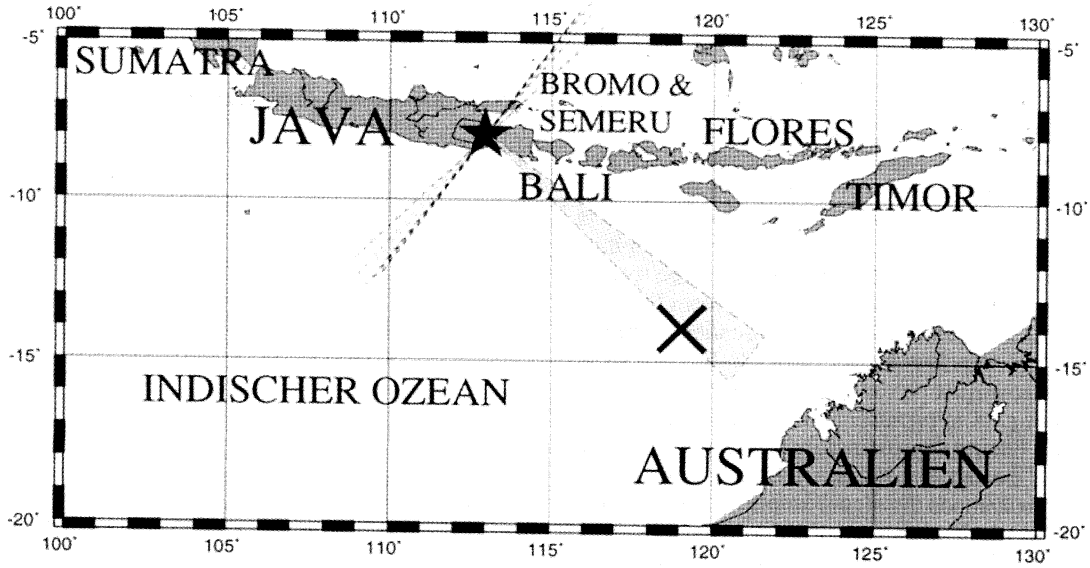

Fig. 11. Direction of the incoming wavefront for the signals between 0.22 and 0.5 Hz. The Tengger national park is indicated by a star. The wave fronts are depicted as dashed lines. The triangle describes the area in which the waves are created. The cross indicates the position of a storm center on December 4 (information from: Meteorological and Geophysical Agency, Jakarta).

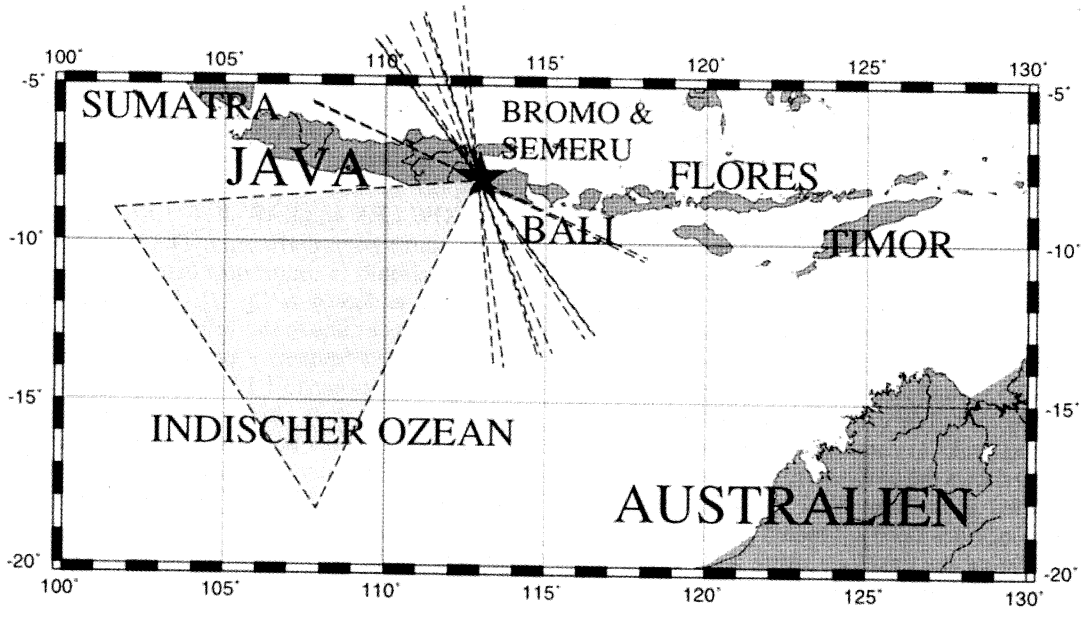

Fig. 12. Same as fig. 11 for the signals between 0.1 and 0.2 Hz.

wave propagation azimuth has been estimated between N 25°E and N 85°E and is shown in fig. 12. The velocity in this frequency band could be on an average determined to 1.5 km/s.

4.3. *Long-period data – frequencies below 0.1 Hz*

Superimposed on the strong tremor activity long-period signals (periods of 100 s and longer) can be found on the seismograms which last for several hours (fig. 4). They can be found throughout the whole recording period though their amplitudes are strongest on December 04 with up to $\pm 10^{-4}$ m/s on the horizontal components. This low frequency activity is about 100 times stronger on horizontal than on vertical components for the same time period.

The fact that the long-period signals are much stronger on the horizontal components leads to the assumption that they are due to ground tilt.

Take $u_z(t)$ to be the vertical displacement. When neglecting second-order (and higher) terms of the tilt component, the vertical acceleration of the seismometer-mass can be expressed as

$$s_z(t) = -\ddot{u}_z(t). \tag{4.1}$$

For the horizontal accelerations $s_x(t)$ and $s_y(t)$ a first-order tilt component has to be considered additionally and we receive for the horizontal accelerations of the mass

$$s_x(t) = -\ddot{u}_x(t) + g\tau_x(t) \tag{4.2}$$

$$s_y(t) = -\ddot{u}_y(t) + g\tau_y(t) \tag{4.3}$$

where $u_x(t)$ and $u_y(t)$ are the horizontal displacements, g is the gravitational constant and τ_x and τ_y describe the angle of horizontal tilt.

As seen from eq. (4.1) tilt signals should not be found at all on the vertical component. As the amplitude of the long-period signals is about a factor 100 smaller on the vertical component, the signal on the vertical component could simply be caused by incorrect levels of the sensor. If an inclination of the vertical sensor by about 0.5 degrees with respect to the vertical is assumed, the signal on the vertical component can be explained by tilt as well.

The tilt has to increase linearly, if a constant velocity of translation is apparently measured. The tilt rate $\dot{\tau}$ can be calculated for periods below T_0 and assuming no horizontal displacement using

$$\dot{\tau} = \frac{\omega_0^2}{g} v \tag{4.4}$$

where $\omega_0 = 2\pi/T_0$ is the angular-eigen-frequency of the seismometer and g is the surface gravity. Assuming a velocity of $v = 5 \cdot 10^{-5}$ m/s for 45 min as it can be seen on station LAW on December 4 between 10 and 11 UT (fig. 4) this

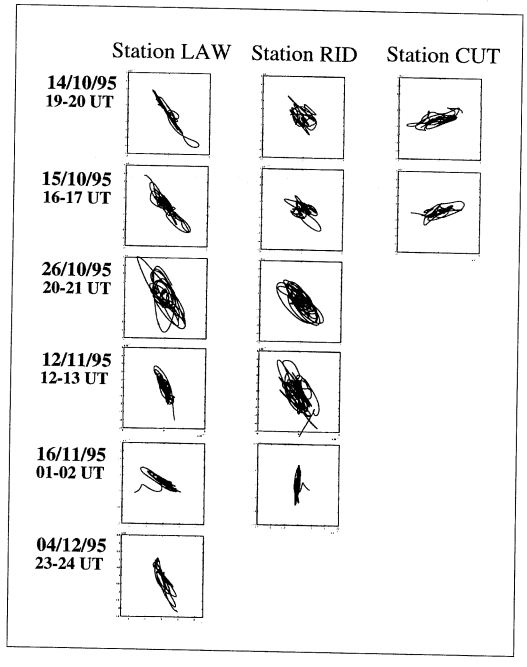

Fig. 13. Particle motion analysis. Each particle motion was calculated of a one-hour-long time series after application of a low-pass filter (0.01 Hz). Starting from the top the single rows diplay data recorded on October 14 between 19 and 20 UT, on October 15 (16-17 UT), on October 26 (20-21 UT), on November 12 (12-13 UT), on November 16 (01-02 UT), and on December 4 (23-24 UT). Columns from left to right correspond to the stations LAW, RID and CUT, respectively. One prefered direction of polarization can be determined for each station.

results in a total tilt $\tau = 3.8 \cdot 10^{-5}$ rad, an amount corresponding to an uplift (or downfall) of 3.8 mm over a baseline of 100 m and easily possible near a volcano in an active state.

A particle motion analysis was performed for the long-period signals, after low-pass filtering the data with 0.01 Hz. Figure 13 shows particle motion diagrams in the horizontal plane for time series one hour long for each day and each station, when data was available. At each station the main direction of polarization points in the same direction. Transferring the main direction of polarization for each station on a map it can clearly be seen that the lines point to the crater-region (fig. 14, dotted lines). This, and the stationarity of the directions can hence be taken as good evidence for the volcanic origin of the tilts.

In detail, the particle motion is either directed *towards* or *away* from the crater on all stations synchronously. This becomes evident when analysing the polarization of shorter time series as shown in fig. 14. Particle motion has been calculated for a three-minute long segment on October 14. Particle motion goes in the direction of the arrows at the stations. At all three stations the arrow first points away from the crater, then towards it and afterwards away again. This points to an inflation-deflation mechanism as a source of these long-period tilts.

The size and the depth of the source can be estimated assuming a sphere-shaped source with radius a which is situated at depth f in an elastic half-space (Mogi, 1958). The pressure p inside the sphere is determined by the lithostatic pressure. A sudden pressure change Δp inside the

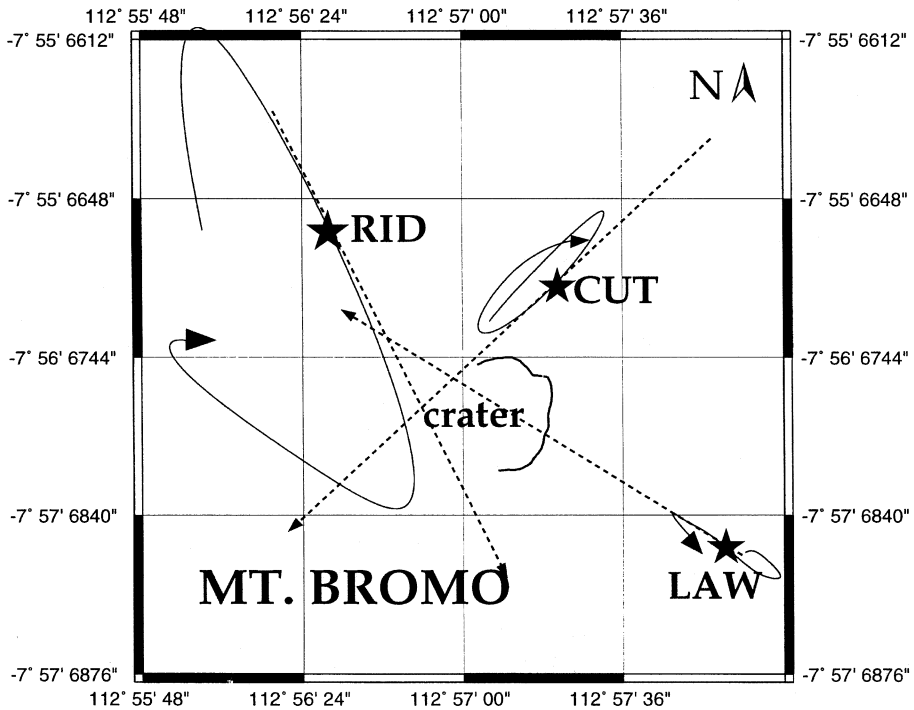

Fig. 14. Map of Mt. Bromo crater region. The positions of the stations are indicated by stars (★). The dotted lines show the main direction of horizontal polarization at each station; the solid lines show the particle motions during a three minute long time window on October 14 (02:07,5-02:10,5 UT).

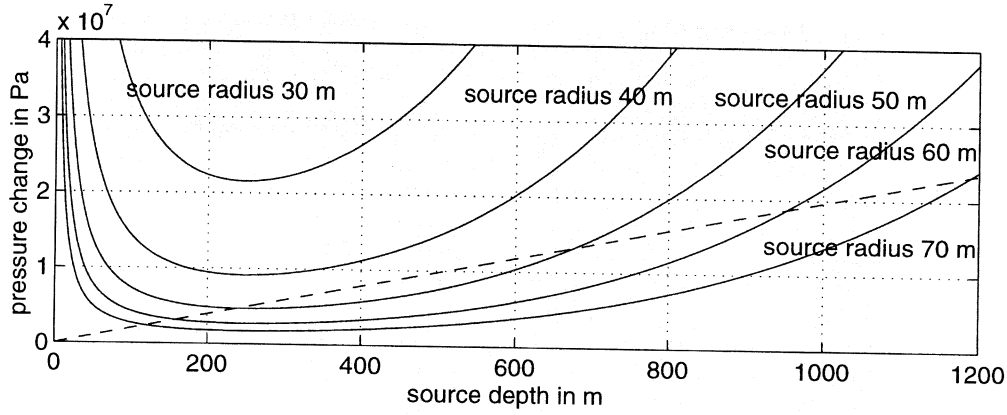

Fig. 15. Pressure change *versus* source depth for different source radii (solid lines). The shear modulus has been set to $6 \cdot 10^8$ Pa. For the distance between source and station a value of 900 m has been taken. The dotted line indicates the lithostatic pressure.

sphere leads to a displacement u at the surface and hence at the recording stations. If the radius of the sphere is much smaller than the depth of the source and Poisson's ratio equals 0.25 then the surface displacement in horizontal direction is given by

$$u_x = \frac{3}{4} \cdot \frac{a^3 \cdot \Delta p}{\mu} \cdot \frac{b}{(f^2 + b^2)^{\frac{3}{2}}} \qquad (4.5)$$

where b is the horizontal distance from the source to the receiver and μ is the shear modulus. Derivating eq. (4.5) with respect to f and solving it for the pressure change Δp results in

$$\Delta p = \frac{4}{3} \cdot \frac{\tau \mu}{a^3} \cdot \frac{(f^2 + b^2)^{\frac{5}{2}}}{-3fb} \qquad (4.6)$$

where the tilt τ is the derivative of the horizontal displacement $\frac{du_x}{df}$. It can be calculated from the seismograms using eq. (4.4). For modelling the source an averaged value of $\tau = 5 \cdot 10^{-6}$ has been used. For the wave velocity inside the Caldera a value of 1 km/s was assumed and the density was assumed to have a value of 2 g/cm^3 (wet sand (Kuchling, 1991)) resulting in a shear modulus $\mu = 6 \cdot 10^{-8}$ Pa. The distance b has been measured as the distance between the stations and the point of intersection from fig. 14.

For a smaller source radius the pressure change required to receive a certain value of tilt τ has to be larger.

The solid lines in fig. 15 show the pressure change for different fixed radii *a versus* source depth *f*. The dotted line indicates the lithostatic pressure.

It is assumed that the pressure change within the sphere is smaller than the lithostatic pressure. Otherwise a pressure-change would lead to an extrusion of volcanic material. Therefore, the source radius can have a maximum value of 50 m. The depth of the source can in this case be restriced to the region between 250 and 650 m. For a source radius of 70 m the source was found in a region between 100 and 1200 m depth. Going back to the assumption that the source radius has to be be much smaller than the source depth, it seems reasonable to assume source depths of at least 500 m in this model.

4.4. *High-frequency tremor – frequency range above 10 Hz*

On December 4 when the low frequency signals became very strong, a tremor signal with high frequencies up to 25 Hz was recorded

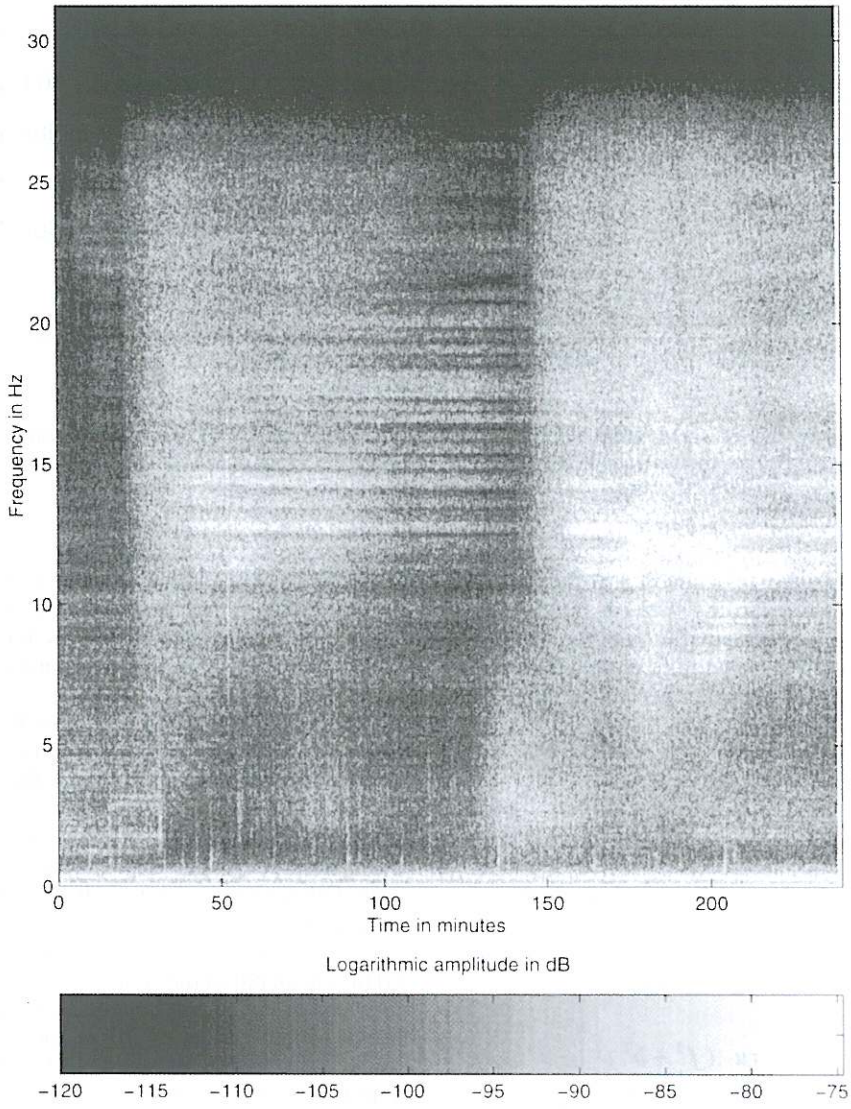

Fig. 16. Spectrogram for December 4, Station LAW, Z-Component. On the time scale three hours are displayed starting from 8 UT. The frequency axis covers the complete range up to the Nyquist-frequency at 31.25 Hz. High amplitudes are found between 10 and 20 Hz.

(fig. 16). The high frequency signal does not appear on all stations simultaneously. Therefore, and because of its high frequency content it is probably related to a shallow or local source rather than to a source deep within the volcano.

In addition to the normal tremor, the transition between high and low amplitudes in this case appears to happen smoothly with a slowly increasing amplitude (fig. 4, middle).

5. Interpretation

Due to their frequency content, the signals recorded at Mt. Bromo can be divided into four classes. The lowest frequency range contains volcanic tilt signals with periods larger than 10 s. Above 1 Hz two classes of volcanic tremor signals can be found of which the first consists of frequencies between 1 and 10 Hz and the latter has a spectral content above 10 Hz. Intermediate, at frequencies from 0.1 to 1 Hz, the data consist of signals that are due to marine microseism and therefore not related to the volcanic activity.

In this class two spectral peaks are dominant. The first sharp peak consists of frequencies between 0.1 and 0.2 Hz and probably is linked to microseism produced at the coastline of Java as shown by the direction of the arriving wavefront which reaches the stations from south-western direction. This signal was observed during the whole recording time. The second peak between 0.3 and 0.4 Hz could only be found during some days around December 4 and October 26. Determination of the direction of wave propagation and an estimation of the phase velocity using the tripartite method show that this signal originates from the region south-east of Mt. Bromo, and that the source is located in the Indian ocean between Java and Australia. A comparison with satellite photos made available by the Meteorological and Geophysical Agency, Jakarta support the assumption. Large storm centers are present around the region of origin. A phase velocity of 1.1 km/s could indicate a participation of surface waves.

The remaining three classes of seismic signals are of volcanic origin. However, the generating source for the different types of volcanic signals does not necessarily have to be identical.

The high frequency tremor requires a local source, because these signals have only been observed at single stations and during a limited time. The distance between source and recording station has to be much smaller than the distance between the three stations, because otherwise the signals should be recorded at more than one station at a time. Hence, source depths larger than a few tens of meters seem to be impossible. Exact location of the sources is, however, not possible. A possible explanation for these signals could be local extrusions of gas or other local phenomena.

The low frequency signals originate from greater depths. They could be generated by slowly rising magma or gas that pushes on the walls of a conduit causing the volcano to bulge. The source has been modelled as a sphere that inflates due to a pressure change. The received tilt signals can only be observed if the source depth is greater than 500 m and if the diameter of the source has a maximum size of 50 m assuming a pressure change smaller than the hydrostatic pressure at a given depth. Polarization analyses reveals a source location near the northwestern edge of the crater at the point of intersection in fig. 14. The total tilt in a period of 45 m could be calculated to $\tau = 3.8 \cdot 10^{-5}$ rad, corresponding to an uplift or downfall of 3.8 mm over a baseline of 100 m.

The source of the 1-10 Hz tremor signals is located close to the point from where the long-period signals originate. The signals could be generated by gas flow through a system of pipes or small cracks resulting in a broad spectrum of frequencies. The broad spectrum could also result from bubbles rising up inside the fluid. These bubbles are formed as a result of decreasing hydrostatic pressure. The models are supported by visual observations during the experiment when gas and steam eruptions frequently were seen. Seismic signals of phase A with high amplitudes were accompanied by strong ash cloud eruptions whereas during phase B (with low tremor amplitudes, respectively), steam clouds dominated. During phase A the pressure of the extruding gas is assumed to be higher giving rise to high amplitudes in the seismogram. On its way through the conduits the gas might take material with it resulting in ash eruptions during this phase. During phases of low amplitudes the gas pressure is not sufficient to move material particles, leading to pure steam emissions during phase B. As the source is located in approximately the same distance to all three stations no restrictions about the source depth can be made. On Bromo the tremor spectra are composed of smaller peaks, which do not show consistency for the different stations. For

that reason they must be affected by the path or the subsoil close to the recording site rather than by an oscillating source.

The peak in the spectrum at 1.25 Hz appeared exclusively during phase A, but it was not always present during this phase. This is not surprising as the feeding conduits inside the volcano may undergo spatial and temporal changes. Throughout the experiment the peak at 1.25 Hz has only been observed during several days around mid November. Nevertheless this spectral peak has also been reported before, for a short time in March 1995 and in early September 1995 (Triastuty, 1997) in a different experiment using 1-Hz-seismometers. The single peak could be produced by a resonating tube or conduit fed by magma or gas for a limited time as proposed in a model by Dahm (1991).

6. Discussion

The results presented show that the spectra of the volcanic signals recorded on Mt. Bromo cover a very broad frequency range. The seismic signals can be classified into four frequency regions.

Tremor signals can be found within the traditional frequency range above 1 Hz. Between 1 and 10 Hz continuous tremor could be found which consists of two different phases distinguished by the amplitude of the signal. The transition between the two phases takes place within a few minutes and is recorded on all stations simultaneously. Within each phase the envelope of the amplitude has a nearly constant value. The source of this tremor signal is found in the northwestern edge of the crater.

Tremor signals above 10 Hz could only be found for a limited time on single stations. These signals might belong to local sources with source depths less than a few tens of meters.

Below 1 Hz remarkable long-period signals are observed. Their amplitudes amount to $\pm 10^4$ m/s. The signals are probably due to tilt because the amplitudes are about 100 times stronger on the horizontal components. Modelling the source as a sudden pressure change in a sphere results in a source depth of at least 500 m.

Apart from the volcanic signals two other signals could be observed which are produced by marine microseism. They could be discriminated from the volcanic signals due to the existence of additional stations at Mt. Semeru about 20 km south of Mt. Bromo.

Acknowledgements

I would like to thank Prof. R. Schick and Dr. W. Zürn for many helpful discussions, for suggesting several improvements and for critically reading the manuscript. I am grateful to Prof. E. Wielandt for his comments and suggestions that helped to improve the paper. Special thanks are due to Dr. J. Neuberg for fruitful discussions and, together with D. Francis, for making available the data and for helping with the data processing. Furthermore I would like to thank Dr. R. Widmer for his constructive comments. This project could not have been realized without the assistance during the fieldwork of many members from the Universities of Leeds (U.K.), Grenoble (France) and Stuttgart (Germany) and members of the Volcanological Survey of Indonesia (Bandung). The project was financially supported by the European Commission, Bruxelles.

REFERENCES

BENOIT, J.P. and S.R. MCNUTT (1997): New constraints on source processes of volcanic tremor at Arenal Volcano, Costa Rica, using broadband seismic data, *Geophys. Res. Lett.*, **24**, 449-452.

DAHM, T. (1991): Eigenvibrations of magma-filled dyke systems with complex geometry, *Volcanic Tremor and Magma Flow*, 97-114.

DREIER, R., R. WIDMER, R. SCHICK and W. ZÜRN (1994): Stacking of broad-band seismograms of shocks at Stromboli, *Acta Vulcanol.*, **5**, 165-172.

GOTTSCHÄMMER, E. (1998): Seismische Signale am Vulkan Bromo, Indonesien, *Diploma Thesis*, Physics Faculty, University of Karlsruhe.

KIRCHDÖRFER, M. (1999): Analysis and quasistatic FE modelling of long period impulsive events associated with explosions at Stromboli volcano (Italy), *Ann. Geofis.*, **42** (3), 379-390 (this volume).

KNOPOFF, L., M.J. BERRY and F.A. SCHWAB (1967): Tripartite phase velocity observations in laterally heterogeneous regions, *J. Geophys. Res.*, **72** (10), 2595-2601.

KUCHLING, H. (1991): Taschenbuch der Physik, *Verlag Harri Deutsch*, Thun und Frankfurt am Main, 13. korr. Auflage.

MCNUTT, S.R. (1994): Volcanic tremor from around the world: 1992 update, *Acta Vulcanol.*, **5**, 197-200.

MOGI, K. (1958): Relations between the eruptions of various volcanoes and the deformation of the ground surfaces around them, *Bull. Earthquake Res. Inst.*, **36**, 99-134.

MOHNEN, J.U. and R. SCHICK (1996): The spatial amplitude distribution of volcanic tremor at Stromboli volcano (Italy), *Ann. Geofis.*, **39** (2), 361-375.

NEUBERG, J. and P.S. WAHYUDI (1991): Study on characteristics and origin of volcanic seismic signals, *Volcanic Tremor and Magma Flow,* 149-163.

NEUBERG, J., R. LUCKETT, M. RIPEPE and T. BRAUN (1994): Highlights from a seismic braodband array on Stromboli volcano, *Geophys. Res. Lett.*, **21**, 749-752.

SCHLINDWEIN, V., J. WASSERMANN and F. SCHERBAUM (1995): Spectral analysis of harmonic tremor signals at Mt. Semeru volcano, Indonesia, *Geophys. Res. Lett.*, **22**, 1685-1688.

TRIASTUTY, H. (1997): Physical analysis on the volcanic activity stages of Mt. Bromo based on tremor spectral analysis and hypocenters of volcanic earthquakes, *S1-Thesis*, Volcanological Survey of Indonesia, Bandung.

WIELANDT, E. and T. FORBRIGER (1999): Near-field seismic displacement and tilt associated with the explosive activity of Stromboli, *Ann. Geofis.*, **42** (3), 407-416 (this volume).

WUNDERMAN, R., E. VENZKE and G. KYSAR (1995a): Tengger Caldera (Bromo) SO_2 and tremor, *Smithsonian Institution, Global Volcanism Network Bulletin*, **20** (3).

WUNDERMAN, R., E. VENZKE and G. KYSAR (1995b): Tengger Caldera (Bromo) ash plume and tremor, *Smithsonian Institution, Global Volcanism Network Bulletin*, **20** (10).